

Destruction of spin cycloid in (111) c -oriented BiFeO₃ thin films by epitaxial constraint: Enhanced polarization and release of latent magnetization

Feiming Bai, Junling Wang, M. Wuttig, JieFang Li, Naigang Wang, A. P. Pyatakov, A. K. Zvezdin, L. E. Cross, and D. Viehland

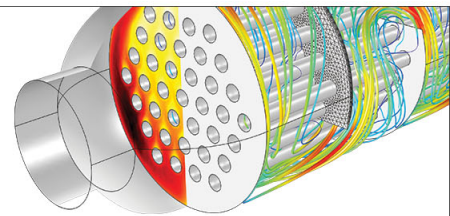
Citation: [Applied Physics Letters](#) **86**, 032511 (2005); doi: 10.1063/1.1851612

View online: <http://dx.doi.org/10.1063/1.1851612>

View Table of Contents: <http://scitation.aip.org/content/aip/journal/apl/86/3?ver=pdfcov>

Published by the [AIP Publishing](#)

Over **700** papers &
presentations on
multiphysics simulation



[VIEW NOW ►](#)

 COMSOL

Destruction of spin cycloid in (111)_c-oriented BiFeO₃ thin films by epitaxial constraint: Enhanced polarization and release of latent magnetization

Feiming Bai^{a)}

Department of Materials Science and Engineering, Virginia Tech, Blacksburg, Virginia 24061

Junling Wang and M. Wuttig

Department of Materials and Nuclear Engineering, University of Maryland, College Park, Maryland 20742

JieFang Li and Naigang Wang

Department of Materials Science and Engineering, Virginia Tech, Blacksburg, Virginia 24061

A. P. Pyatakov and A. K. Zvezdin

Institute of General Physics, Russian Academy of Science, Vavilova St., 38, Moscow 119991, Russia

L. E. Cross

Materials Research Institute, Pennsylvania State University, State College, Pennsylvania 16802

D. Viehland

Department of Materials Science and Engineering, Virginia Tech, Blacksburg, Virginia 24061

(Received 20 August 2004; accepted 16 November 2004; published online 14 January 2005)

In BiFeO₃ films, it has been found that epitaxial constraint results in the destruction of a space modulated spin structure. For (111)_c films, relative to corresponding bulk crystals, it is shown (i) that the induced magnetization is enhanced at low applied fields; (ii) that the polarization is dramatically enhanced; whereas, (iii) the lattice structure for (111)_c films and crystals is nearly identical. Our results evidence that epitaxial constraint induces a transition between cycloidal and homogeneous antiferromagnetic spin states, releasing a latent antiferromagnetic component locked within the cycloid. © 2005 American Institute of Physics. [DOI: 10.1063/1.1851612]

Multiferroic materials have more than one order parameters.^{1,2} In magnetoelectric materials, they are a spontaneous polarization P_s and a spontaneous magnetization M_s .¹ Of particular interest is BiFeO₃ (BFO), which exhibits the coexistence of ferroelectric and antiferromagnetic (G-type) orders up to quite high temperatures.^{1,3} The average structure of BiFeO₃ crystals is a distorted rhombohedral perovskite,^{3–11} which belongs to the space group $R3c$ (or C_6^{3V}). The rhombohedral unit cell parameters are $a_r = 5.634 \text{ \AA}$ and $\alpha_r = 59.348^\circ$.⁷ The pseudo-cubic representation of these rhombohedral cell parameters is $a_c = 3.963 \text{ \AA}$ and $\alpha_c = 89.40^\circ$. In this structure, the pseudo-cubic (111)_c is equivalent to hexagonal (001)_h. The Bi³⁺ and Fe³⁺ cations are displaced from their centro-symmetric positions along [111]_c. This distortion is polar and results in a P_s oriented along (111)_c of $P_{(111)c} = 0.061 \text{ C/m}^2$. BiFeO₃ also has antiferromagnetic order along (001)_h/(111)_c.^{10,12} The antiferromagnetic spin order is not homogenous, rather a space modulated one.¹¹ It is manifested as an incommensurate cycloid structure with a wavelength λ of $\sim 620 \text{ \AA}$ along [110]_h.^{11,13} The antiferromagnetic vector is locked within the cycloid, averaged to zero over λ .^{14,15}

This latent magnetization can be released by application of high magnetic fields.¹⁶ Recent electron spin resonance investigations have also shown an induced phase transition from cycloidal to homogeneous antiferromagnetic spin orders for $H > 18 \text{ T}$.¹⁷ This induced phase transition can be

understood by the following Landau–Ginzburg (LG) theory:^{14–18}

$$F_{\text{homogeneous}} < F_{\text{cycloid}}, \quad (1a)$$

$$F_{\text{cycloid}} = -\frac{1}{4A}(\gamma \cdot P_z)^2 + \frac{K_u}{2} - \frac{\chi_{\perp}(\beta \cdot P_z)^2}{4} - \frac{K_{\text{pert}}}{2}, \quad (1b)$$

$$F_{\text{Homogenous}} = K_u - \chi_{\perp} \frac{(\beta \cdot P_s)^2}{2} - K_{\text{pert}}, \quad (1c)$$

where β is the magnetoelectric (ME) constant of the homogeneous antiferromagnetic spin state; K_u is the uniaxial magnetic anisotropy, P_z is the spontaneous polarization along z , γ is the inhomogeneous magnetoelectric constant, and χ_{\perp} is the magnetic susceptibility in the direction the perpendicular to the antiferromagnetic vector. In Eq. (1) above, we have also included a perturbation term K_{pert} , which will be discussed below.

Recently, dramatically increased values of remanent polarization P_r have been reported in epitaxial thin films of BiFeO₃ grown on (001)_cSrTiO₃.¹⁹ For example, the P_r of (001)_cBiFeO₃ thin films is $\sim 55 \mu\text{C/cm}^2$ —which is $\sim 10\times$ larger than that of a bulk crystal projected onto the same orientation. Clearly, epitaxial heterostructure can induce significant and important changes. *This letter is focused on (111)_c films—we will show that epitaxial constraint may destroy the spin cycloid, resulting in the release of the latent magnetization. This is achieved without notable change in crystal structure.*

Phase pure BiFeO₃ thin films have been grown with a 2000 Å thickness by pulsed laser deposition onto (111)_c

^{a)} Author to whom correspondence should be addressed; electronic mail: fbai@vt.edu

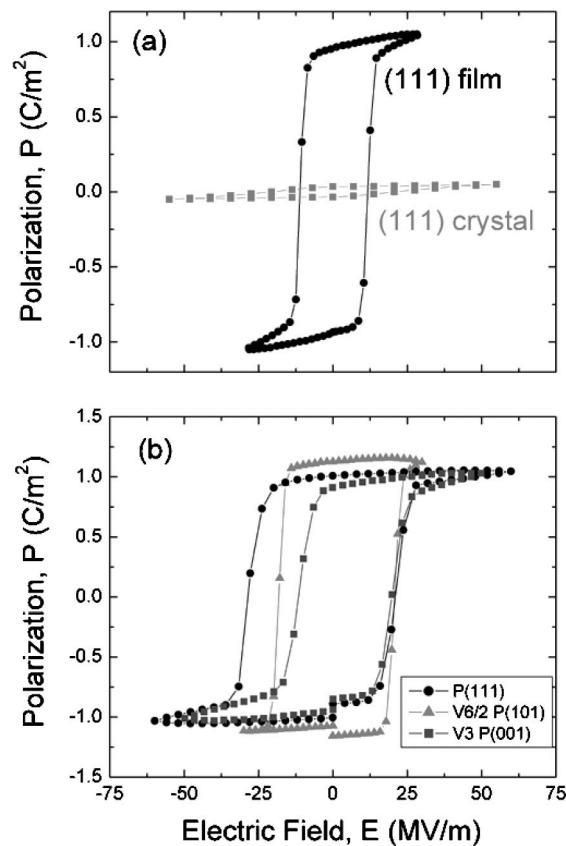


FIG. 1. Ferroelectric properties for BiFeO₃ films. (a) P - E curve for (111)_c-oriented film, including corresponding data for bulk crystal; and (b) P - E curves for (001)_c, (101)_c, and (111)_c films projected onto (111)_c.

single crystal SrTiO₃ substrates. Additional films have been grown on (001)_c and (110)_c SrTiO₃ for supplementary studies. A conducting perovskite oxide, SrRuO₃ (SRO),²⁰ was chosen as the bottom electrode due to the slight lattice mismatch with the BFO structure. A SRO layer of 500 Å was deposited at 600 °C in an oxygen ambient of 100 mTorr, and followed by the BFO film, deposited at 670 °C in an oxygen ambient of 20 mTorr at a growth rate of 0.7 Å/s. Chemical analysis was carried out by scanning electron microscopy x-ray microanalysis, indicating a cation stoichiometry of ~1:1 in BFO films.²¹ X-ray diffraction studies were performed using a Philips MPD system. Ferroelectric measurements were performed using a RT6000 test system (Radiant Technologies). The dc magnetization (i.e., M - H response) was characterized as a function of H at various temperatures using a superconducting quantum interference device magnetometer (Quantum Design, model XL7).

First, the values of the interplanar spacing of (111)_c epitaxial thin layers were measured by x-ray diffraction, and compared to those of a (111)_c oriented bulk crystal; 2 θ - ω mesh scans of (111), (110), and (100) films were obtained (data not shown). Calculations revealed that the films have a rhombohedral structure, with a lattice spacing of $d_{(001)} = 3.959$ Å. This is very close to that of the bulk single crystal.

Next, we investigated the effect of the constrained crystallographic film state on the ferroelectric properties of BiFeO₃. The ferroelectric properties were characterized by a polarization hysteresis method. Figure 1(a) shows the P - E response for the (111)_c film. We observed hysteresis loops

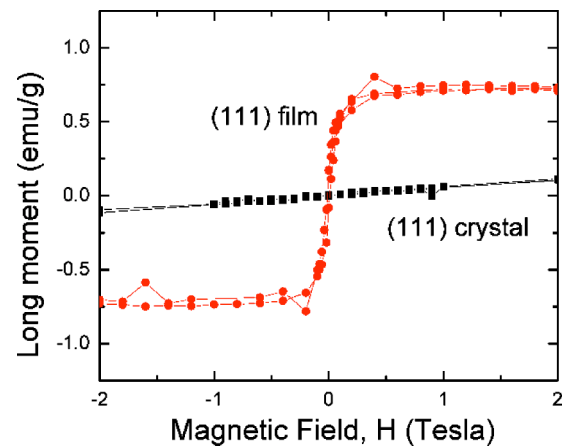


FIG. 2. Magnetization properties for (111)_cBiFeO₃ films and corresponding crystal.

typical of a ferroelectric, with a remanent polarization P_r of ~1 C/m². Corresponding measurements of a bulk crystal are also shown in the figure for comparisons. In addition, we have measured the orientation dependence of P_r . Figure 1(b) shows $\sqrt{3}P_{(001)c}$, $\sqrt{6}/2P_{(101)c}$, and $P_{(111)c}$ as a function of E for variously oriented films. In this figure, the values of the projected polarizations can be seen to be nearly equivalent. This confirms that the direction of spontaneous polarization lies close to (111)_c, and that the values measured along (101)_c and (001)_c are simply projections onto these orientations. Clearly, similar to bulk crystals, the spontaneous polarization is oriented close to (111)_c. However, P_s is dramatically increased!

Finally, the M - H properties of the films were also characterized, as shown in Fig. 2. In this figure, it can be seen that the induced magnetization is on an order of 0.6 emu/g. This is much higher than that of (111)_c bulk crystal, which was measured over the same magnetic field range of $H_{ac} = 2$ T, as shown in the figure for comparisons. However, it is close to the expected value of M_s induced in bulk crystals at the cycloidal to homogenous antiferromagnetic spin transition field of $H \cong 18$ T.¹⁶ For our films, it is also important to note (i) the lack of hysteresis in the M - H response; (ii) the low magnetic field at which spin rearrangement occurs, $H < 10^3$ Oe; and (iii) the relatively high magnetic susceptibility.

Our results show (i) that the structure of (111)_c BiFeO₃ thin films is essentially identical to that of bulk crystals; (ii) that the polarization is dramatically increased relative to the bulk crystal; and (iii) the presence of an induced magnetization at low magnetic fields, which is somewhat close to that of a homogeneous antiferromagnetic spin state.¹⁶ It is important to note that no structural phase changes were found to accompany the changes in the polarization and magnetization.

For (111)_cBiFeO₃ thin layers, these results indicate that the cycloidal spin structure is destroyed by a critical perturbation provided by the elastic constraint of the film and that a homogenous antiferromagnetic spin state is stabilized. We attempt to understand the influence of epitaxy on the LG formalism by adding a rhombic perturbation of K_{pert} to the uniaxial magnetic anisotropy K_u , which we had originally included in Eq. (1) above. A phase transition from the cycloidal to the homogeneous antiferromagnetic spin states will

occur in Eq. (1) at a critical value of the perturbation K_{pert}^c , when the energy of the cycloidal state is equal to that of the homogeneous one. This will occur when the anisotropy constant fulfills the critical perturbation condition of

$$K_{\text{pert}}^c > \frac{(\gamma \cdot P_s)^2}{2A} + K_u - \chi_{\perp} \frac{(\beta \cdot P_s)^2}{2} \\ \approx 2 \times 10^6 \frac{\text{erg}}{\text{cm}^3} = 2 \times 10^5 \frac{\text{J}}{\text{m}^3}, \quad (2)$$

where $\chi_{\perp} = 4.7 \times 10^{-5}$, A is the stiffness constant, $A = 3 \times 10^{-7} \text{ erg/cm}$, $\gamma \cdot P_s = 2Aq$, q is the wave vector of the modulation, $q = 2\pi/\lambda$, $\lambda = 620 \text{ \AA}$, $K_u = 6.6 \times 10^5 \text{ erg/cm}^3$ and $\beta \cdot P_s = 1.2 \times 10^5 \text{ Oe}$.^{17,19} Thus, a transition to a uniform antiferromagnetic spin state will occur if the critical anisotropy perturbation is $K_{\text{pert}}^c \approx 10^6 \text{ erg/cm}^3$ or 10^5 J/m^3 .

One possible source for a perturbation greater than K_{pert}^c is a piezoelectric-magnetolectric bi-effect. We estimate Young's modulus as $Y = 10^{11} \text{ N/m}^2$, by comparisons with other complex ferroelectric perovskites.²² The corresponding mechanical stress is $\sigma = Y \cdot \epsilon_{\text{epi}} \approx 5 \times 10^8 \text{ N/m}^2$ ($\epsilon_{\text{epi}} \approx 0.5\%$), which can induce a polarization change via the piezoelectric effect of $P = d\sigma \approx 0.05 \text{ C/m}^2 = 5 \mu\text{C/cm}^2$, where $d = 1 \times 10^{-10} \text{ C/N}$ is the piezoelectric constant.¹⁹ Due to magnetolectric coupling, this induced polarization then gives rise to a magnetic field of $H_{\text{ME}} = \beta \cdot P \approx 2 \times 10^5 \text{ Oe}$, where $\beta = 1/\alpha_p$ and $\alpha_p \approx 3 \times 10^{-7} \text{ C/(m}^2 \cdot \text{Oe)}$ (this value of the α_p can be calculated from the magnetization induced by the electric field of the spontaneous polarization in bulk BiFeO_3 crystals,¹⁷ which is in agreement with that reported for (001) films¹⁶). This yields a contribution of $\chi_{\perp} H_{\text{ME}} \approx 10^6 \text{ erg/cm}^3$ (or 10^5 J/m^3) to the magnetic anisotropy. This is of the same order as that by the critical perturbation condition K_{pert}^c . Thus, an in-plane epitaxial constraint in (111)_c BiFeO_3 thin films is sufficient to break the cycloidal spin order, and in so doing releasing the latent magnetization locked within the cycloid. This is achieved solely by a magnetolectric coupling between polarization and magnetization, mediated by elastic constraint. However, recently, we have obtained much higher saturation magnetizations ($\sim 2 \text{ emu/g}$) in (001)-oriented BiFeO_3 ultrathin films, where we observed that M_s increases with decreasing film thickness: investigations of this excess magnetization for (001) films will be done in the future.

In summary, BiFeO_3 films grown on (111)_c have a rhombohedral structure, essentially identical to that of single crystals. The easy axis of spontaneous polarization lies close to (111)_c. Our results evidence that epitaxial constraint induces

a transition between cycloidal and homogeneous antiferromagnetic spin states, releasing a latent antiferromagnetic component locked within the cycloid, via magnetolectric exchange.

The authors are pleased to acknowledge support from the office of Naval Research (ONR) under Contract Nos. MURI N000140110761, N000140210340, N000140210126, NSF-MRSEC under Contract No. DMR-00-80008, and RFBF Grant Nos. 05-02-16997-a, 04-02-81046-Bel2004.

¹G. A. Smolenskii and I. Chupis, *Sov. Phys. Usp.* **25**, 475 (1982).

²E. K. H. Salje, *Phase Transitions in Ferroelastic and Co-Elastic Crystals: An Introduction for Mineralogists, Material Scientists, and Physicists* (Cambridge University Press, Cambridge, 1990), p. 147.

³S. V. Kiselev, R. P. Ozerov, and G. S. Zhdanov, *Sov. Phys. Dokl.* **7**, 742 (1963).

⁴Yu. N. Venetsev, G. Zhdanov, and S. Solov'ev, *Sov. Phys. Crystallogr.* **4**, 538 (1960).

⁵G. Smolenskii, V. Isupov, A. Agranovskaya, and N. Krainik, *Sov. Phys. Solid State* **2**, 2651 (1961).

⁶Yu. E. Roginskaya, Yu. Ya. Tomashpol'skii, Yu. N. Venetsev, V. M. Petrov, and G. S. Zhdanov, *Sov. Phys. JETP* **23**, 47 (1966).

⁷F. Kubel and H. Schmid, *Acta Crystallogr., Sect. B: Struct. Sci.* **46**, 698 (1990).

⁸C. Michel, J-M. Moreau, G. D. Achenbach, R. Gerson, and W. J. James, *Solid State Commun.* **7**, 701 (1969).

⁹J. D. Bucci, B. K. Robertson, and W. J. James, *J. Appl. Crystallogr.* **5**, 187 (1972).

¹⁰J. R. Teague, R. Gerson, and W. J. James, *Solid State Commun.* **8**, 1073 (1970).

¹¹I. Sosnowska, T. Peterlin-Neumaier, and E. Steichele, *J. Phys. C* **15**, 4835 (1982).

¹²G. Smolenskii, V. Yudin, E. Sher, and Yu. E. Stolypin, *Sov. Phys. JETP* **16**, 622 (1963).

¹³I. Sosnowska, M. Loewenhaupt, W. I. F. David, and R. Ibberson, *Physica B* **180-181**, 117 (1992).

¹⁴Yu. F. Popov, A. Zvezdin, G. Vorob'ev, A. Kadomtseva, V. Murashev, and D. Rakov, *JETP Lett.* **57**, 69 (1993).

¹⁵Yu. F. Popov, A. Kadomtseva, S. Krotov, D. Belov, G. Vorob'ev, P. Makhov, and A. Zvezdin, *Low Temp. Phys.* **27**, 478 (2001).

¹⁶A. Kadomtseva, A. Zvezdin, Y. Popov, A. Pyatakov, and G. Vorob'ev, *JETP Lett.* **79**, 571 (2004).

¹⁷B. Ruetter, S. Zvyagin, A. Pyatakov, A. Bush, J. F. Li, V. Belotelov, A. Zvezdin, and D. Viehland, *Phys. Rev. B* **69**, 064114 (2004).

¹⁸A. Kadomtseva, Yu. Popov, G. Vorob'ev, and A. Zvezdin, *Physica B* **211**, 327 (1995).

¹⁹J. Wang, J. Neaton, H. Zheng, V. Nagarajan, S. Ogale, B. Liu, D. Viehland, V. Vaithyanathan, D. Schlom, U. Waghmare, N. Spaldin, K. Rabe, M. Wuttig, and R. Ramesh, *Science* **299**, 1719 (2003).

²⁰C. Eom, R. J. Cava, R. Fleming, and J. Phillips, *Science* **258**, 1766 (1992).

²¹S. Chantrell and E. P. Wohlfarth, *J. Magn. Magn. Mater.* **40**, 1 (1983).

²²D. Viehland, F. Tito, E. McLaughlin, H. Robinson, R. Janus, L. Ewart, and J. Powers, *J. Appl. Phys.* **90**, 1496 (2001).